Inorg. Chem. **2002**, *41*, 4417−4423

Density Functional Calculations for Modeling the Oxidized States of the Active Site of Nickel–Iron Hydrogenases. 1. Verification of the Method with Paramagnetic Ni and Co Complexes

Christian Stadler, Antonio L. de Lacey, Belén Hernández, Víctor M. Fernández,* and Jose C. Conesa*

Instituto de Catálisis y Petroleoquímica, CSIC, Campus Universidad Autónoma, 28049 Madrid, Spain

Received January 4, 2002

ZORA relativistic DFT calculations are presented which aim to reproduce geometric structures and EPR properties of $[Ni(mnt)_2]^-$ (H_2mnt = maleonitrildithiol), two other paramagnetic low-spin Ni(III) complexes, and an asymmetric paramagnetic Co(II) complex. The study tests the accuracy of the computational method as a prior step to the modeling of the geometric and electronic structure of the active site of NiFe hydrogenases in its EPR-active oxidized states Ni-A and Ni-B. Systematic deviations from experiment are found for the calculated *g*-values; relative differences among them are, however, well reproduced. Because no significant improvements have been achieved by using larger basis sets or more sophisticated functionals, *g*-values may be calculated rather rapidly at the VWN level. This is most important for the modeling of the active site of NiFe hydrogenases because its complexity does not permit calculations at high levels of theory. For $[Ni(mnt)_2]^-$, excellent agreement between calculated and experimental results is obtained for the ^{14}N quadrupole coupling, whereas the calculated hyperfine couplings are not always in good agreement with experimental data.

Introduction

Enzymes that catalyze the reversible oxidation of molecular hydrogen are called hydrogenases. Besides containing several iron atoms, many of them contain a redox active nickel ion.[1] Many aspects of the enzyme operation mechanism and the underlying electronic structure features are ill understood, so that their elucidation by theoretical methods is of great interest. Several density functional (DFT) studies on the active site of these enzymes have been published recently.[2] However, the various computational models differ considerably, and none of the proposed mechanisms has been generally accepted.

It seems that most of the DFT approaches used so far are not very sensitive toward small changes of geometric and/or electronic structure. Besides geometric parameters, the energetics of hydrogen activation[2a,b,e,i] and the infrared frequencies of the diatomic ligands bound to the Fe center[2e−g] have been used to verify the computational models. On the other hand, some of the best characterized properties of these enzymes are the parameters obtained by EPR (and ENDOR) spectroscopy.[1,3] These are very closely related to the electronic structure and are expected to depend sensitively on the protonation state, which cannot be determined from X-ray diffraction data. However, the theoretical calculation of *g*-tensors is not trivial. For decades, simple second-order perturbation theory has been used, which can be applied to either semiempirical or ab initio calculations but has

* To whom correspondence should be addressed. E-mail: vmfernandez@icp.csic.es (V.M.F.); jcconesa@icp.csic.es (J.C.C.).

(1) (a) Cammack, R.; Fernandez, V. M.; Schneider, K. In *The Bioinorganic Chemistry of Nickel*; Lancaster, J. R., Jr., Ed.; VCH: Weinheim, 1988; pp 167−190. (b) Moura, J. J. G.; Teixeira, M.; Moura, I.; LeGall, J. In *The Bioinorganic Chemistry of Nickel*; Lancaster, J. R., Jr., Ed.; VCH: Weinheim, 1988; pp 191−226. (c) Albracht, S. P. J. *Biochim. Biophys. Acta* **1994**, *1188*, 167−204.

(2) (a) Pavlov, M.; Siegbahn, P. E. M.; Blomberg, M. R. A.; Crabtree, R. H. *J. Am. Chem. Soc.* **1998**, *120*, 548−555. (b) Pavlov, M.; Blomberg, M. R. A.; Siegbahn, P. E. M. *Int. J. Quantum Chem.* **1999**, *73*, 197−207. (c) De Gioia, L.; Fantucci, P.; Guigliarelli, B.; Bertrand, P. *Inorg. Chem.* **1999**, *38*, 2658−2662. (d) De Gioia, L.; Fantucci, P.; Guigliarelli, B.; Bertrand, P. *Int. J. Quantum Chem.* **1999**, *73*, 187−195. (e) Niu, S.; Thomson, L. M.; Hall, M. B. *J. Am. Chem. Soc.* **1999**, *121*, 4000−4007. (f) Amara, P.; Volbeda, A.; Fontecilla-Camps, J. C.; Field, M. J. *J. Am. Chem. Soc.* **1999**, *121*, 4468−4477. (g) Li, S.; Hall, M. B. *Inorg. Chem.* **2001**, *40*, 18−24. (h) Stein, M.; Lubitz, W. *Phys. Chem. Chem. Phys.* **2001**, *3*, 2668−2675.

(3) (a) Moura, J. J. G.; Moura, I.; Huynh, B.-H.; Krüger, H. J.; Teixeira, M.; DuVarney, R. C.; DerVartanian, D. V.; Xavier, A. V.; Peck, H. D., Jr.; LeGall, J. *Biochem. Biophys. Res. Commun.* **1982**, *108*, 1388−1393. (b) Cammack, R.; Patil, O. S.; Hatchikian, E. C.; Fernandez, V. M. *Biochim. Biophys. Acta* **1987**, *912*, 98−109.

10.1021/ic020015t CCC: $22.00
Published on Web 07/31/2002

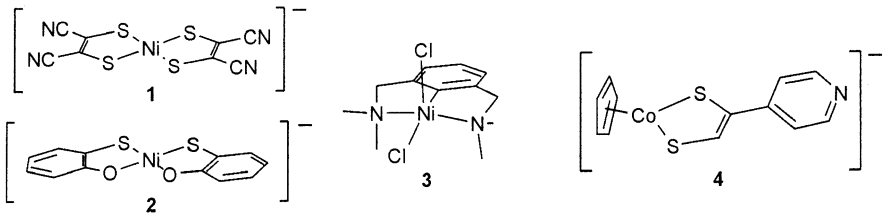

Figure 1. Schematic representations of the model complexes **1**−**4** used in the calculations. Hydrogen atoms are not shown.

shortcomings as it requires, among other things, a good evaluation of electronic excitation energies.[4] More recently, a more sophisticated approach, still within a perturbation theory scheme, has been used by Schreckenbach et al. but has not yet been implemented in commercially available software.[5]

An alternative for systems with one unpaired electron has been developed by van Lenthe et al. in which the spin−orbit interaction was included in the Hamiltonian of a spin-restricted relativistic DFT method.[6] The currently available implementation of this method allows for the calculation of *g*-tensors as well as of the parameters quantifying the hyperfine coupling (*A*-tensors)[7] and nuclear quadrupole interactions (*P*-tensors)[8] that can be determined experimentally by EPR and ENDOR techniques. Until recently, this method has been applied only to some small model compounds and a handful of transition metal complexes,[6,9] most of them of the simple d^1 type. During the preparation of this manuscript, however, a first study on two paramagnetic Ni complexes (one Ni(III) and one Ni(I)) using the same method appeared,[10] followed by another study by the same group on active site models of NiFe hydrogenases.[11] In the present paper, we primarily test whether paramagnetic Ni(III) complexes containing heavy ligands, and especially their EPR parameters, can be described properly with this new DFT method, as it is generally considered that the so-called Ni-A and Ni-B states of the active site of NiFe hydrogenases, for which EPR/ENDOR parameters have been determined in detail, are Ni(III) states.[1,3] In addition, we present calculations of a low symmetry paramagnetic Co complex, as the active site of these enzymes is asymmetric.[12] To get an idea of the accuracy of the obtained values and their dependence on (a) the size of the basis set, (b) the density functional, and (c) the geometrical data, we have performed extensive calculations on the Ni and Co complexes given in Figure 1: the planar anions $[Ni(mnt)_2]^-$ (H_2mnt = maleonitriledithiol) (**1**) and $[Ni(mp)_2]^-$ (H_2mp = 2-mercaptophenol) (**2**), the five-coordinated neutral complex $Ni(NCN')Cl_2$ (NCN' = $C_6H_3(CH_2NMe_2)_2$-*o*,*o*') (**3**), and the anionic cobalt complex $[CpCo(dith)]^-$ (Cp = cyclopentadienyl and dith = pyridin-4-yl-ene-1,2-dithiolate) (**4**). Calculated geometries and *g*-tensors as well as hyperfine and quadrupole couplings are compared with available experimental data.

Methods

All calculations were done with the Amsterdam density functional (ADF) program package[13] using Slater-type orbitals and the ZORA (zeroth-order regular approximation) relativistic method.[14] The different parameters used to evaluate the computational models require slightly different computational approaches. Particularly, the two components of the hyperfine coupling tensor *A*, namely the isotropic (scalar) component a_{iso} and the anisotropic component *T*, are taken here from different calculations, as will be explained in more detail later. Scalar relativistic calculations were carried out employing either spin-restricted (open shell) wave functions (in geometry optimizations) or spin-unrestricted wave functions (mainly for the determination of isotropic hyperfine couplings a_{iso}, but also for that of spin densities, which are taken from a Mulliken population analysis, and quadrupole couplings). On the other hand, the calculations of *g*- and *T*-tensors, which included spin−orbit interactions, employed spin-restricted (open shell) wave functions exclusively.

A double-ζ basis set without polarization functions was used in most of the spin-restricted calculations. Here, it is referred to as basis A or A′ depending on the treatment of nonvalence orbitals: in the former, the core orbitals are frozen, whereas the latter is a full electron basis set. A larger basis set, which is triple-ζ throughout and includes one polarization function for all atoms except Ni and Co, was also used, primarily in the spin-unrestricted calculations; it is further referred to as basis set B (frozen cores) or B′ (full electron). These basis sets A/A′ and B/B′ are those designated in ADF as standard basis sets II and IV, respectively.[15]

The density functionals employed are all based on the VWN local density functional parametrized by Vosko et al.[16] BLYP[17,18]

(4) Abragam, A.; Bleany, B. *Electron Paramagnetic Resonance of Transition Ions*; Clarendon: Oxford, 1970; Chapter 15.

(5) (a) Schreckenbach, G.; Ziegler, T. *J. Phys. Chem. A* **1997**, *101*, 3388−3399. (b) Schreckenbach, G.; Ziegler, T. *Theor. Chem. Acc.* **1998**, *99*, 71−82.

(6) van Lenthe, E.; Wormer, P. E. S.; van der Avoird, A. *J. Chem. Phys.* **1997**, *107*, 2488−2498.

(7) van Lenthe, E.; van der Avoird, A.; Wormer, P. E. S. *J. Chem. Phys.* **1998**, *108*, 4783−4796.

(8) van Lenthe, E.; Baerends, E. J. *J. Chem. Phys.* **2000**, *112*, 8279−8292.

(9) (a) Patchkovskii, S.; Ziegler, T. *J. Chem. Phys.* **1999**, *111*, 5730−5740. (b) van Lenthe, E.; van der Avoird, A.; Hagen, W. R.; Reijerse, E. J. *J. Phys. Chem. A* **2000**, *104*, 2070−2077. (c) Patchkovskii, S.; Ziegler, T. *J. Am. Chem. Soc.* **2000**, *122*, 3506−3516. (d) Belanzoni, P.; van Lenthe, E.; Baerends, E. J. *J. Chem. Phys.* **2001**, *114*, 4421−4433.

(10) Stein, M.; van Lenthe, E.; Baerends, E. J.; Lubitz, W. *J. Phys. Chem. A* **2001**, *105*, 416−425.

(11) Stein, M.; van Lenthe, E.; Baerends, E. J.; Lubitz, W. *J. Am. Chem. Soc.* **2001**, *123*, 5839−5840.

(12) (a) Volbeda, A.; Charon, M. H.; Piras, C.; Hatchikian, E. C.; Frey, M.; Fontecilla-Camps, J. C. *Nature* **1995**, *373*, 580−587. (b) Volbeda, A.; Garcin, E.; Piras, C.; De Lacey, A. L.; Fernandez, V. M.; Hatchikian, E. C.; Frey, M.; Fontecilla-Camps, J. C. *J. Am. Chem. Soc.* **1996**, *118*, 12989−12996.

(13) (a) ADF 1999.02 and ADF 2000.02. (b) Fonseca Guerra, C.; Snijders, J. G.; Te Velde, G.; Baerends, E. J. *Theor. Chem. Acc.* **1998**, *99*, 391−403.

(14) van Lenthe, E.; Snijders, J. G.; Baerends, E. J. *J. Chem. Phys.* **1996**, *105*, 6505−6516. (b) van Lenthe, E.; Ehlers, A.; Baerends, E. J. *J. Chem. Phys.* **1999**, *110*, 8943−8953.

(15) Further details can be found at http://www.scm.com/Doc/atomicdata/.

Table 1. Bond Lengths and *g*-Values for $[Ni(mnt)_2]^-$ (**1**) from Spin-Restricted Calculations

		bond lengths [Å]			*g*-values[d]		
geometry	method[a]	Ni−S	S−C1	C1−C1	g_x	g_y	g_z
	exptl[b]	2.147−2.151	1.705−1.727	1.367−1.370	2.14	2.04	1.99
exptl	VWN, A				2.096	2.030	1.977
	VWN, B				2.086	2.029	1.975
symmetrized[c]	VWN, A	2.149	1.720	1.368	2.097	2.030	1.976
	VWN, B				2.086	2.029	1.974
optimized	VWN, A	2.166	1.792	1.370	2.112	2.032	1.979
	VWN, B	2.117	1.719	1.380	2.077	2.029	1.974

[a] A, B refer to the basis set used. [b] The bond lengths have been taken from ref 20b. The *g*-values given are those measured in a frozen solution of **1** in DMSO/$CHCl_3$.[20c] [c] The distances given here are those obtained by symmetrization of the experimental data referred to previously. [d] The g_z principal direction coincides with the normal to the molecule plane, while the g_y direction is perpendicular to the symmetry plane which does not intersect the ligands.

and BP (Becke−Perdew)[17,19] gradient corrections were also tested. Additional details about the computational parameters are given in the corresponding subsections.

Detailed structural and EPR data are available for the anions $[Ni(mnt)_2]^-$ (H_2mnt = maleonitrildithiol) (**1**)[20] and $[Ni(mp)_2]^-$ (H_2-mp = 2-mercaptophenol) (**2**).[21] The neutral complex [Ni(NCN′)-Cl_2] (NCN′ = $C_6H_3(CH_2NMe_2)_2$-*o*,*o*′) (**3**) has been also characterized by EPR spectroscopy, but structural data are only known for the analogous iodine derivative.[22,23] All three complexes can be regarded as Ni(III) d^7 low-spin systems with one unpaired electron and can thus be treated within the spin-restricted formalism. Because the X-ray structures of these complexes show only small deviations from idealized symmetry, most calculations have been performed on symmetrized geometries (D_{2h}, C_{2v}, and C_s for **1**, **2**, and **3**, respectively) that were obtained from the experimental ones using a utility included in the Cerius2 program package.[24]

EPR data of $[CpCodith]^-$ (4) are used which were obtained in tetraethylene glycol frozen solution (77 K).[25] X-ray data were not accessible, and consequently, a model construction was employed as starting point for a full geometry optimization. The energetically minimized structure was then used for the EPR calculations.

Results and Discussion

$[Ni(mnt)_2]^-$. $[Ni(mnt)_2]^-$ (**1**) has been experimentally characterized in full detail in (frozen) solution and in the crystalline state (as (Et_4N)- and (*n*-Bu_4N)-salt). Besides the *g*-values, the principal values of the *A*-tensors of ^{61}Ni and all ligand atoms (for the nuclei ^{13}C, ^{14}N, ^{15}N, and ^{33}S) are known.[20,26] The hyperfine tensors have been studied by Hayes, using a DFT method different from ours;[27] very recently, also the ZORA method used in the present work was applied to complex **1** by Stein et al.[10] Our first aim here was to find the least costly way of calculating accurate structural and magnetic resonance parameters (in order to apply the same procedure to the much bigger models of the hydrogenase active site). Consequently, the results presented later are similar but not identical to those of Stein et al., who used mainly large full electron basis sets.

Geometric Structure. Selected bond lengths taken from the experimental structure and from the corresponding symmetrized one are compared with calculated values in Table 1. Symmetrization clearly does not change the relevant geometric characteristics (nor does it affect the *g*-values). Consequently, the geometry optimizations were carried out on D_{2h} symmetric structures. In these optimizations, a significant effect was found when changing the size of the basis set or the density functional. Without gradient corrections, basis set A already yields acceptable agreement with experimental data. Particularly, the Ni−S bond length, which is most important for the resulting *g*-values, is calculated well. On the other hand, the bigger basis set B yields a Ni−S bond length that is clearly too short.

It is well-known that the inclusion of gradient corrections improves the accuracy of DFT calculations in terms of thermodynamic properties, for example, bonding energies. Usually, it also leads to better bond lengths and thus to a more accurate molecular geometry. We tested the BLYP and BP gradient-corrected functionals and found substantially longer bond lengths (data not shown) than in the corresponding calculations without gradient corrections, which reflects a well-known trend.[28] However, the Ni−S bond length is calculated to be too long when gradient corrections are included, particularly with basis set A. Actually, the combination of the VWN local density functional and basis set A yields geometric data that are almost as close to the experimental data (the average deviation is 0.03 Å in bond lengths and 0.6° in angles) as the best values obtained with

(16) Vosko, S. H.; Wilk, L.; Nusair, M. *Can. J. Phys.* **1980**, *58*, 1200−1211.
(17) Becke, A. D. *Phys. Rev. A* **1988**, *38*, 3098−3100.
(18) (a) Lee, C.; Yang, W.; Parr, R. G. *Phys. Rev. B* **1988**, *37*, 785−789. (b) Russo, T. V.; Martin, R. L.; Hay, P. J. *J. Chem. Phys.* **1994**, *101*, 7729−7737.
(19) Perdew, J. P. *Phys. Rev. B* **1986**, *33*, 8822−8824.
(20) (a) Maki, A. H.; Edelstein, N.; Davison, A.; Holm, R. H. *J. Am. Chem. Soc.* **1964**, *86*, 4580−4587. (b) Kobayashi, A.; Sasaki, Y. *Bull. Chem. Soc. Jpn.* **1977**, *50*, 2650−6. (c) Huyett, J. E.; Choudhury, S. B.; Eichhorn, D. E.; Bryngelson, P. A.; Maroney, M. J.; Hoffman, B. M. *Inorg. Chem.* **1998**, *37*, 1361−1367.
(21) (a) Balch, A. L. *J. Am. Chem. Soc.* **1969**, *91*, 1948−1953. (b) Köckerling, M.; Henkel, G. *Chem. Ber.* **1993**, *126*, 951−953. (c) Chou, J.-H.; Varotsis, C.; Kanatzidis, M. G. In *Bioinorganic Chemistry. An Inorganic Perspective of Life*; Kessissoglou, D. P., Ed.; NATO ASI Series C; Kluwer Academic Publishers: Dordrecht, The Netherlands, 1995; Vol. 459, pp 333−348.
(22) (a) Grove, D. M.; van Koten, G.; Zoet, R.; Murall, N. W.; Welch, A. J. *J. Am. Chem. Soc.* **1983**, *105*, 1380−1381. (b) Grove, D. M.; van Koten, G.; Mul, P.; Zoet, R.; Linden, J. G. M.; Legters, J.; Schmitz, J. E. J.; Murall, N. W.; Welch, A. J. *Inorg. Chem.* **1988**, *27*, 2466−2473.
(23) Preliminary calculations on the iodine complex soon revealed that the method is much less accurate here, probably because of the presence of such a heavy atom as iodine, and were thus not pursued further.
(24) *Cerius2 molecular modeling system*; Molecular Simulations Inc.: San Diego, CA, 1999.
(25) Mabbs, F. E.; Collison, D. *Electron Paramagnetic Resonance of Transition Metal Compounds;* Studies in Inorganic Chemistry 16; Elsevier Science Publishers: Amsterdam, 1992; p 249.
(26) (a) Davison, A.; Edelstein, N.; Holm, R. H.; Maki, A. H. *J. Am. Chem. Soc.* **1963**, *85*, 2029−2030. (b) Schmitt, R. D.; Maki, A. H. *J. Am. Chem. Soc.* **1968**, *90*, 2288−2292.
(27) Hayes, R. G. *Inorg. Chem.* **2000**, *39*, 156−158.
(28) Ziegler, T. *Chem. Rev.* **1991**, *91*, 651−667.

gradient corrections (using basis set B and BLYP). Besides, it is much less costly with respect to the computational effort.

Comparison with recent work shows that a slight improvement of some of the calculated structural parameters, particularly the S−C1 bond length, can be achieved using a combination of a large full electron basis set and the BP functional.[10] However, the resulting effect on calculated *g*-values (see later) and the electronic structure is small and, from our point of view, does not justify the dramatic increase of computation time that will result when larger and/or less symmetric structures, for example, hydrogenase active site models or complexes **3** and **4**, have to be calculated.

***g*-Values.** The calculated electronic structure is fully coincident with that described in great detail by Stein et al.;[10] that is, the SOMO is largely delocalized over the four sulfur atoms and the central Ni atom (mainly in its d_{yz} orbital, as already proposed by Maki et al.[20a]). Examining Table 1, we find that virtually identical *g*-values are calculated for the symmetrized and the experimental structure. Although it is well-known that *g*-values are very sensitive to structural changes, the result is not surprising in this case given the small deviation of the X-ray structure from D_{2h} symmetry. This justifies our decision to use a symmetric starting structure in the geometry optimizations. Table 1 further demonstrates that, within the VWN local density method, the smaller basis set A systematically yields higher (and thus better) *g*-values than basis set B, in agreement with previous work.[10] In the case of the two optimized structures, the differences are particularly big because the calculated Ni−S distances are very different.

The inclusion of gradient corrections generally did not improve the *g*-values. Only small improvements of 0.002−0.006 were found for g_x. This is in full accordance with earlier results, which indicated that the use of the small basis set A and the VWN functional yields satisfying results regarding both geometries and *g*-values.[9a,c] Also, the use of the frozen core approximation does not affect the *g*-values: we found differences smaller than 0.001 between full electron basis sets A′ and B′ and basis sets A and B, respectively. Therefore, most of the spin-restricted calculations described later, either within the spin−orbit or the scalar relativistic approach (for *g*- and *T*-tensor calculations and for geometry optimizations, respectively), were done at this computational level (VWN and basis set A), which performs equally well as the method chosen by Stein et al. (BP and a large full electron basis set).[10]

One important result to be noted is that all calculated *g*-values in Table 1 are smaller than the experimental values. This is most pronounced for g_x, which was expected because it shows the greatest deviation Δg from the free electron value $g_e = 2.0023$. However, the relative error, which we may define as $[1 - (\Delta g^{calcd}/\Delta g^{exptl})] \times 100\%$, is similar for g_x and g_y ($\geq 21\%$). Note that the value g_z does not follow that rule: it is calculated to be significantly smaller than the free electron value although the experimental value is rather close to g_e. Still, the agreement with the experiment can be considered remarkably good for all three *g*-values in view of the results recently obtained with the same method for another planar d^7 system, an iron(I) porphyrin.[9b]

Hyperfine Coupling. The *A*-tensor, which describes the hyperfine coupling interaction between the unpaired electron and a nucleus with noninteger spin *I*, can be decomposed in an isotropic and an anisotropic component, referred to as a_{iso} and the *T*-tensor, respectively.[29] The isotropic component, which is a simple scalar that can be calculated as the arithmetic average of the principal values A_i of the *A*-tensor, depends on the spin density at the nucleus whereas the anisotropic component (the traceless tensor *T*) results from a dipolar interaction between the magnetic moments of the electron and the nucleus. This implies that the latter component is likely to be calculated well using the frozen core approximation, whereas the former requires an accurate description of the inner shells.

As will be discussed in following paragraphs, the anisotropic hyperfine coupling can be obtained in the same spin−orbit calculations as the *g*-values. In fact, we found that, at least in the case of Ni, it is not well calculated in spin-unrestricted scalar relativistic calculations (data not shown), where the effect of spin−orbit coupling, which determines the deviation of the electron magnetic moment from the free electron value, is not considered. On the other hand, the isotropic hyperfine coupling a_{iso} is not well calculated within the spin-restricted formalism.[10,30] Therefore, spin-unrestricted calculations were performed on the optimized structure of complex **1**. The a_{iso} values in Table 2 were calculated with the full electron basis set B′, which performed considerably better than basis set A′ whereas no further improvement was obtained when a second polarization function was added to the ligand atoms (data not shown). We decided to use the gradient-corrected BP functional in the spin-unrestricted calculations because it showed the best overall performance in agreement with earlier work.[30]

For a_{iso} of nickel and the carbon atoms, good agreement with experiment is obtained. The experimental value of a_{iso}-(^{33}S) is unknown but can be estimated from the principal values of the *A*-tensor yielding ±5.2 or ±23.3 MHz, depending on the choice of signs for the three principal values. In earlier works, equal signs were proposed for the three values leading to $a_{iso} = \pm 23.3$ MHz and a total spin density at the four sulfur atoms of approximately 0.55.[9c,26b] However, in recent DFT studies, much better agreement with experiment was found for the alternative assignment of signs.[10,27] Our calculated total spin density of 0.64 reproduces satisfactorily the mentioned experimentally derived value (0.55)[9c,26b] and is identical to the value found by Stein et al.[10] However, Table 2 shows that a_{iso} is calculated much too small. Trying the other geometries in Table 1, we noticed that this value is virtually independent of the geometric parameters. However, we found that it is significantly bigger (1.6 MHz) when the BLYP functional is used instead of BP, although BP clearly yields better agreement for all nuclei

(29) For the principal values, the following relations apply: $T_1 + T_2 + T_3 = 0$; $A_i = a_{iso} + T_i$; $i = 1, 2, 3$.

(30) Belanzoni, P.; Baerends, E. J.; Gribnau, M. *J. Phys. Chem. A* **1999**, *103*, 3732−3744.

Table 2. Calculated and Experimental Hyperfine Coupling Data for $[Ni(mnt)_2]^-$ (**1**)[a,b]

	a_{iso} [MHz]			*T*-tensor [MHz]		*A*-tensor [MHz]		
nucleus	BP	exptl	ref	VWN	exptl	calcd	exptl	ref
^{61}Ni	17.5	**13** ± **3**[c]	26a	(26.0, −5.3, −20.7)	(29, −8, −21)[d]	(43.5, 12.2, −3.2)	(**45**, **8**, <**6**)	20a
^{33}S	0.6	**5.2**[e]		(*−12.8*, *−11.5*, 24.3)	(−18.8, −18.8, 37.6)[e]	(*−12.2*, *−10.9*, 24.9)	(**13.5**, **13.5**, **43**)	26b
^{13}C1	−2.8	−2.1	20c	(*−2.6*, *−2.3*, 4.9)	(−2.5, −2.5, 5.0)	(*−5.4*, *−5.1*, 2.1)	(−4.6, −4.6, 3.0)[f]	20c
^{13}C2	−2.2	−2.9	20c	(*−0.4*, *0.7*, −0.3)	(0.3, 0.1, −0.4)[g]	(*−2.6*, *−1.5*, −2.5)	(−2.6, −2.8, −3.4)[f]	20c
^{14}N	0.1	0.4	20c	(*−0.6*, *−0.4*, 1.0)	(−0.26, −0.29, 0.55)	(*−0.5*, *−0.3*, 1.1)	(0.13, 0.10, 0.94)	20c

[a] The calculations are based on the geometry optimized using basis set A and the VWN functional. a_{iso} values were taken from gradient-corrected spin-unrestricted calculations using basis set B′. Principal values of the *T*-tensor were taken from spin-restricted spin−orbit calculations without gradient corrections using basis set A. [b] Bold numbers indicate that the sign could not be determined experimentally. An italicized number indicates that the axis of the calculated *T*- or *A*-tensor does not coincide with the corresponding *g*-tensor axis. [c] Measured in liquid solution. [d] T_x and T_y are calculated from the experimental data for A_x, A_y (assumed to be of equal sign; otherwise no agreement with calculations results) and a value of $a_{iso} = 16$ MHz. With $a_{iso} < 16$ MHz, no consistency of experimental data is found; that is, one would have $|A_z| > 6$ MHz, and $a_{iso} > 16$ MHz deviates too much from the experimental value in liquid solution.[26a] T_z then is chosen such that a traceless *T*-tensor results. This yields $A_z = -5$ MHz, compatible with the experimental results. [e] The given values were calculated under the assumption of opposite signs for the axial and equatorial components of the experimental *A*-tensor. [f] Actually, opposite signs for the values A_i were reported by Huyett et al.,[20c] but they are not consistent with their values of a_{iso} and the *T*-tensor. [g] The given T_i values were recalculated from the experimental A_i values because the values reported by Huyett et al.[20c] are not internally consistent.

other than sulfur. In any case, agreement with experiment is not satisfying. Probably, the a_{iso} values, being strongly conditioned by the spin polarization of the innermost orbitals, depend critically on the accuracy with which the density functionals represent exchange interactions at high electron densities. The different accuracy of the a_{iso} values obtained for ^{61}Ni and ^{33}S suggests that the symmetry of the local interelectron interactions, which determine the orbital polarization contributions to the overall spin density, is also of great importance.

We have to conclude that, even with the gradient-corrected functionals now available to us, we cannot reliably calculate the isotropic hyperfine coupling for all nuclei with good accuracy. We are aware that Stein et al. reported a better, but still not very accurate, value for $a_{iso}(^{33}S)$ using a nonstandard homemade basis set with an added tight 1s function for Ni and S.[10] We could reproduce their value of 3.1 MHz using this basis set, made available to us by E. van Lenthe, but we would like to point out that the agreement for ^{61}Ni then becomes worse, also when applied to hydrogenase active site models.[31] This approach thus does not generally solve the problem.

Table 2 shows that the anisotropic component, that is, the *T*-tensor, is calculated quite well for the Ni atom and the ethylenic carbon atoms C1. For the two atoms of the cyano group, the agreement with experiment is worse. Naturally, these very small anisotropic couplings are especially susceptible to small errors. This has already been pointed out by Hayes.[27] Significant deviation from experiment is also found for the *T*-tensor of ^{33}S. As pointed out previously, the isotropic coupling a_{iso} of ^{33}S has not been determined experimentally, but the calculations strongly support the smaller of the two possible values. This implies an "experimental" *T*-tensor as given in Table 2. Clearly, the three resulting values are bigger than those calculated. Again, we verified that the calculated values do not significantly depend on the geometrical and computational parameters. Actually, our values are similar to those reported by Stein et al.,[10] despite the different basis sets and density functionals.

(31) See companion paper: Stadler, C.; De Lacey, A. L.; Montet, Y.; Volbeda, A.; Fontecilla-Camps, J. C.; Conesa, J. C.; Fernandez, V. M. *Inorg. Chem.* **2002**, *41*, 4424−4434.

One possible explanation for the observed deviation of computed *T*-tensors from experiment is the effect of spin-polarization, which is not included. It has been shown, however, that this contribution is small for the nuclei in complex **1**.[10] The isotropic and anisotropic components a_{iso} and T_i calculated for complex **1** can be combined and then compared with the experimentally observed hyperfine coupling represented by the *A*-tensor's principal values. As a consequence of the discussed discrepancies and uncertainties, only for Ni and C1 is good agreement found (Table 2).

Quadrupole Coupling. Finally, the nuclear quadrupole interaction with the nitrogen atoms should be examined. Experimentally, the *P*-tensor was found to be almost axial with principal values $P(1, 2, 3) = (-1.95, 0.85, 1.10)$ MHz; the smaller positive component is perpendicular to the molecular plane, and the negative component is oriented along the CN bond.[20c] From the spin-unrestricted calculation with basis set B′, we obtain a similarly oriented tensor with $P(1, 2, 3) = (-1.95, 0.79, 1.16)$ MHz in excellent agreement with experiment. It should be mentioned that the use of the frozen core approximation is not recommendable here, as already pointed out by van Lenthe et al.[8] In the present case, the principal values of the *P*-tensor are clearly calculated to be too small when the core orbitals of nitrogen are frozen: for example, we obtain $P(1, 2, 3) = (-1.63, 0.62, 1.01)$ MHz with basis set B. On the other hand, we found that the use of the small basis set A for all non-nitrogen atoms does hardly affect the ^{14}N nuclear quadrupole coupling parameters as long as the nitrogen atoms themselves are treated with basis set B′. Effects of spin−orbit coupling can be neglected: if it is included, the computation time is significantly increased without changing the results.

$[Ni(mp)_2]^-$. Qualitatively, the electronic structure of the anionic complex $[Ni(mp)_2]^-$ (**2**) is similar to that of complex **1**, with the SOMO mainly distributed over the central Ni atom (in the d_{yz} orbital) and the four ligand atoms of the first coordination sphere. However, it shows somewhat different *g*-values because of the different ligand system. Table 3 compares the results obtained for both the symmetrized experimental geometry and the energy minimized geometry with experimental values. First of all, it should be noted that the agreement between experimental and energy-

Table 3. Interatomic Distances and *g*-Values for $[Ni(mp)_2]^-$ (**2**) from Spin-Restricted Calculations[a]

	interatomic distances [Å]				g-values[c]		
geometry	Ni−S	Ni−O	S−S	O−O	g_x	g_y	g_z
exptl data[b]	2.117−2.119	1.849−1.851	3.011	2.597	2.188	2.033	2.014
symmetrized	2.117	1.850	3.010	2.596	2.136	2.020	1.972
optimized	2.156	1.841	3.024	2.597	2.159	2.019	1.974

[a] Basis set A and the VWN functional were employed. [b] The bond lengths have been taken from ref 21b. The *g*-values were measured in a frozen solution of **2** in DMF.[21c] [c] The g_z principal direction is perpendicular to the molecule plane, while the g_x direction bisects the S−Ni−S and O−Ni−O angles.

minimized geometry is generally good. This confirms that basis set A in combination with the VWN local density functional is a good choice for structure determination in the type of systems described in the present paper. Concerning EPR parameters, *g*-values very similar to those shown in Table 3 were obtained with basis set B (data not shown), confirming that the calculated *g*-values are relatively insensitive to the size of the basis set. The differences with experimental values are slightly larger than those observed for $[Ni(mnt)_2]^-$ (**1**) with again all *g*-values calculated to be too small. In particular, g_z is significantly underestimated whereas for the other two values the relative error in Δg is about 30%. The reason for these larger errors remains unclear. One could think of an influence of the molecular symmetry, which is lower in complex **2**; we will comment on this point later. Analysis of the calculated hyperfine couplings cannot clarify the situation because no experimental data are available for comparison; it has only been reported that the ^{61}Ni hyperfine splitting in the EPR spectrum is "insignificant".[21c]

[Ni(NCN')Cl$_2$]. The two anionic complexes discussed previously are rather symmetric four-coordinated systems which are highly delocalized, only about one-third of the unpaired electron being located at the nickel center in a d_{yz} orbital. On the other hand, the oxidized states of NiFe hydrogenases are asymmetric and less delocalized d_{z^2} systems[32] with five ligands[12] coordinated to Ni. Therefore, the C_s-symmetric square-pyramidal complex Ni(NCN')Cl$_2$ (**3**) is of great interest for the further evaluation of the computational method. The experimental *g*-values were reported as $g(x, y, z) = (2.369, 2.195, 2.024)$.[22] These values are amazingly similar to those reported for the oxidized states of NiFe hydrogenases and suggest a low-spin Ni(III) center with the unpaired electron in a d_{z^2} orbital.

We calculated $g(x, y, z) = (2.151, 2.112, 1.998)$ for the fully optimized structure whereas the partial optimization of the two chloro ligands' positions with all remaining atoms fixed at the positions experimentally determined for Ni(NCN')I$_2$ yielded $g(x, y, z) = (2.198, 2.090, 2.001)$. The axes labeling in this system corresponds to having the g_y principal direction normal to the molecule symmetry plane while the g_x direction is roughly coincident with the Ni−C bond. The discrepancy between experimental and calculated *g*-values is rather large (relative error 40−60%), but we do not believe it to be the mere result of bad structural parameters. Most likely, it is the consequence of an insufficiently accurate description of the MO energies, particularly that of the SOMO and the low-lying unoccupied orbitals. This could be due to the chloro ligands which might be modeled less accurately, but also the low molecular symmetry, leading to a mixture of atomic orbitals, might be responsible. Actually, analysis of the SOMO of complex **3** shows that it has significant contributions from $d_{x^2-y^2}$ rather than consisting of a pure d_{z^2} orbital, as already postulated by Grove et al.[22b]

[CpCodith]$^-$. The structure of this low-spin cobalt(II) complex (also a d^7 system) can be observed in Figure 1. It is an anionic low symmetry complex with the metal atom coordinated to the two sulfur atoms from the dith ligand and to one cyclopentadienyl. Because no experimental data in this respect are available, we will skip the discussion of the calculated structural parameters.

***g*-Values.** The experimental *g*-values measured in frozen solution are $g(x, y, z) = (2.235, 2.034, 1.992)$,[25] in the range found for the oxidized states of NiFe hydrogenases. We calculated $g(x, y, z) = (2.110, 2.000, 1.988)$ for the fully optimized structure; here, the g_z principal direction approximately bisects the S−Co−S angle, and the g_y direction is roughly perpendicular to the S−Co−S plane. All three components of the *g*-tensor are underestimated as expected, g_x showing the most important deviation (relative error 46%). Absolute errors for g_y and g_z are considerably smaller. From our point of view, the relative error, as defined previously, is not suitable for discussing these two latter values, because of the proximity of both of them to g_e. Comparing these results with those found for $[Ni(mnt)_2]^-$ and $[Ni(mp)_2]^-$, one observes that the differences between experimental and calculated g_x values are larger for $[CpCo(dith)]^-$, although the g_z component of the tensor is now better reproduced. It is reasonable to assume that differences in molecular symmetry (which is lower in the latter compound) may be to some degree responsible for this different degree of accuracy.

Hyperfine Coupling. Because of the noninteger spin of the only natural isotope ^{58}Co, a clear hyperfine structure is visible in the EPR spectrum of complex **4**. Estimated values are $A(x, y, z) = (281, 17, 75)$ MHz.[25] Because a_{iso} has not been determined independently, nothing is known about the signs of these values. We calculated $a_{iso} = -79$ MHz and $T(x, y, z) = (-170, 124, 46)$ MHz yielding $A(x, y, z) = (-249, 45, -33)$ MHz. If we now use the same signs for the three experimental values A_i, we obtain estimated values $a_{iso} = -113$ MHz and $T(x, y, z) = (-168, 130, 38)$ MHz; other sign combinations lead to worse agreement between computed and experimental values. Clearly, agreement between experiment and calculation is very good for the *T*-tensor, and we must conclude that a_{iso} is computed much

(32) Gessner, Ch.; Trofanchuk, O.; Kawagoe, K.; Higuchi, Y.; Yasuoka, N.; Lubitz, W. *Chem. Phys. Lett.* **1996**, *256*, 518−524.

too small. The reason for this is not really clear, but we believe that a correct description of the isotropic hyperfine coupling is hampered by the fact that the SOMO consists of a mixture of several rather different atomic orbitals. This is a direct consequence of the low molecular symmetry of complex **4** in comparison to complex **1**, where much better agreement with experiment is found for the central metal ion.

Conclusions

Good agreement with experimental structures is obtained for the studied complexes in calculations using basis set A and the VWN functional. In fact, the discrepancies in bond lengths and angles are much smaller than the experimental errors reported for the hydrogenase active site structures, which thus should be well modeled at this level of theory.

Because the *g*-values were always calculated too small for all complexes **1**−**4**, accurate reproduction of the experimental *g*-values of NiFe hydrogenases cannot be expected with active site models. In fact, for g_x and g_y, which are not very close to the free electron value g_e, we expect to find relative errors of at least 20%, so that any observation of smaller deviations should be taken rather as an indication of possibly incorrect theoretical models. On the other hand, the relative errors should be very similar for Ni-A and Ni-B models, which means that the experimental differences in *g*-values between Ni-A and Ni-B should be well reproduced (within this same level of underestimation).

Because the deviation of computed hyperfine coupling parameters from experiment has been shown to be quite large for certain atoms in $[Ni(mnt)_2]^-$ (**1**) and [CpCodith] (**4**), these parameters must be used cautiously for the verification of the active site models. Particularly, the isotropic hyperfine coupling seems to be calculated accurately only in those cases where molecular symmetry leads to simple molecular orbital patterns at the atom concerned. Significantly better agreement is expected with the anisotropic component *T*, although the latter is not always determined experimentally without ambiguity. On the other hand, excellent agreement has been found for the ^{14}N quadrupole coupling in complex **1**, and the same is expected for the modeling of such interactions in the active site of NiFe hydrogenases.

Acknowledgment. This research was supported by Grant BIO4-98-0280 from the European Union BIOTECH program and Grant BQU2000-0991 from the Spanish Ministerio de Ciencia y Tecnología (MCYT). A.L.D. thanks the MCYT for a "Ramon y Cajal" contract. C.S. thanks the German Academic Exchange Service (DAAD) for a postdoctoral fellowship and Dr. Arnd Müller for helpful discussions. We also thank Dr. E. van Lenthe for providing an enlarged basis set.

Supporting Information Available: Coordinates of **1**−**4** optimized with basis set A and the VWN functional (PDF). This material is available free of charge via the Internet at http://pubs.acs.org.

IC020015T